

DEMIXING OF AN INITIALLY HOMOGENEOUS SOLUTION OF PARAMAGNETIC IONS IN INHOMOGENEOUS MAGNETIC FIELDS

YANG¹ X., TSCHULIK² K., UHLEMANN³ M., ODENBACH¹ S., ECKERT¹ K.

¹ Institute of Fluid Mechanics, Chair of Magnetouiddynamics, Measuring and Automation Technology, TU Dresden, D-01069 Dresden, Germany

² Department of Chemistry, Oxford University, Oxford OX1 3QZ, UK

³ Institute for Complex Materials, IFW Dresden, P.O. 270116, 01171 Dresden, Germany

Email: xuegeng.yang@tu-dresden.de

Abstract: Applying interferometry to an aqueous solution of paramagnetic manganese ions, subjected to an inhomogeneous magnetic field, we observe an unexpected but highly reproducible change in the refractive index. This change occurs in the top layer of the solution, closest to the magnet. The shape of the layer is in accord with the spatial distribution of the largest component of the magnetic field gradient force. It turns out that this layer is heavier than the underlying solution because it undergoes a Rayleigh-Taylor instability upon removal of the magnet.

1 Introduction

Magnetic fields were proved to be a useful tool to manipulate objects according to their magnetic properties on macroscale, microscale and occasionally on nanoscale (1)(2). An increasing interest is noticeable in the application of magnetic fields to manipulate of objects according to their magnetic properties. These applications are based on the magnetic field gradient force \vec{f}_m . However, the control of superparamagnetic nanoparticles in magnetic field gradients is a formidable task because the large mean-squared displacement due to Brownian motion makes it difficult for the magnetic field gradient force to track such small particles at all(3)(4). Thus, with a view to the atomic scale, corresponding to paramagnetic ions, any impact of \vec{f}_m was considered even less likely. However, recent study on molecular scale also showed results unexpected from established physical models, for example, the manipulation of single molecular spin or phase separation in dispersion of nanorods, see references in (5).

In the present contribution, we show the opposite of what was stated above: we demonstrate that magnetic ions in a homogeneous aqueous solution can be locally enriched by means of a superimposed magnetic gradient field. This finding is not only of high interest from the theoretical point of view, but is of great importance for a variety of applications, for example, for recycling of rare-earth metals from industrial waste water.

2 Experimental

Paramagnetic MnSO_4 solutions with different concentrations were prepared using analytical grade reagents and deionized water. The total magnetic susceptibility of the solution is given by

$$\chi_{sol} = \sum_k \chi_{mol,k} \cdot C_k \quad (1)$$

where $\chi_{mol,k}$ and C_k refers to the molar susceptibility of the molecules and concentration of sort k . Taking $\chi_{mol, H_2O} \cdot C_{H_2O} = -9 \cdot 10^{-6}$ into account along with the molar susceptibility of

MnSO_4 , $\chi_{mol, \text{MnSO}_4} = 1.678 \times 10^{-7} \text{ m}^3/\text{mol}$ we can derive the susceptibilities of the solutions used. In this way, we find e.g. 1.588×10^{-4} for an 1 M MnSO_4 solution. The homogeneous MnSO_4 solution was injected into the cuboid glass cuvette with an inner side length of 10.0 mm, which was covered by a thin glass cover slip. A cylindrical NdFeB permanent magnet with a diameter of 10.0 mm and a height of 5.0 mm was placed 0.5 mm above the cover slip, see Fig. 1a.

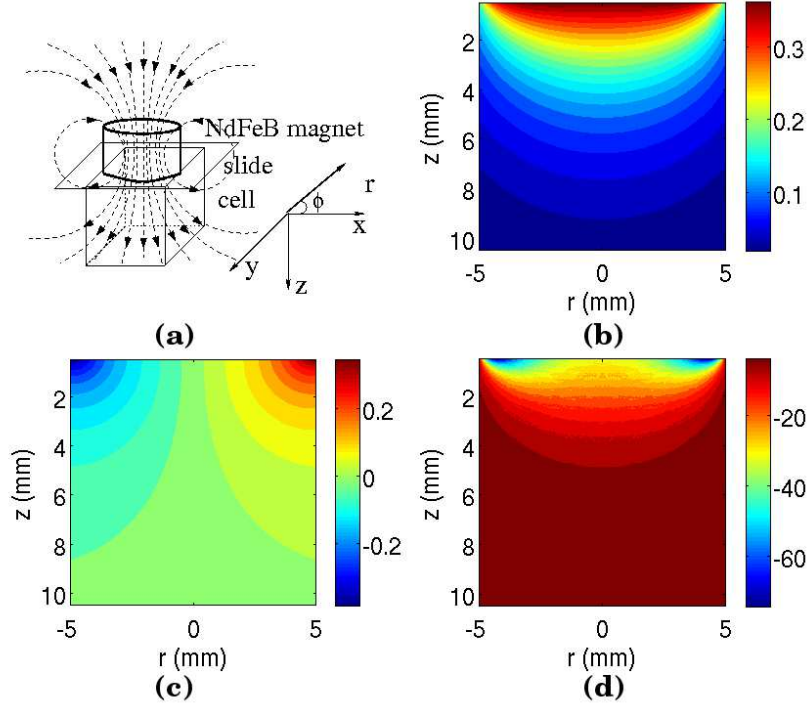


Figure 1: (a) Sketch of magnet and cell setup. (b) and (c) represent B_z and B_r in Tesla. (d) shows the dominant part, $B_z \frac{\partial B_z}{\partial z}$ in T^2/m , of the axial field gradient component according to Eq. 3.

The resulting spatial distribution of the magnetic induction \vec{B} around the magnet was simulated by means of a Finite Element Solver (Amperes 9.0) and is axisymmetric by definition. Hence, the azimuthal component B_ϕ and the respective derivative, $\partial/\partial\phi$ cancel out in the azimuthal direction. As a result, the following components in r and z direction remain in the field gradient force density \vec{f}_m :

$$[(\vec{B} \cdot \nabla)\vec{B}]_r = B_r \frac{\partial B_r}{\partial r} + B_z \frac{\partial B_r}{\partial z} \quad (2)$$

$$[(\vec{B} \cdot \nabla)\vec{B}]_z = B_r \frac{\partial B_z}{\partial r} + B_z \frac{\partial B_z}{\partial z} \quad (3)$$

To intuitively understand the plots in Fig. 1b-d, imagine the magnetic dipole, Fig. 1a. The field lines exit at the magnet's north pole, which immediately faces the solution. Hence, in the upper central part of the solution, B_z is the dominating component (Fig. 1b). By contrast, because of the bending of the field lines towards the opposite south pole, B_r becomes noticeable along the perimeter of the magnet, i.e. at the upper sidewalls of the cuvette, see Fig. 1c. Significant gradients, $\partial B_r/\partial r$, appear only in the corners, while $\partial B_z/\partial z$ also penetrates the upper bulk solution. Thus, one can show that the dominant component in (Eq.2-Eq.3) is $B_z \frac{\partial B_z}{\partial z}$, as plotted

in Fig. 1d.

A Mach-Zehnder interferometer was used to study the evolving concentration distribution of $C_{Mn^{2+}}$ in the cell under the action of f_m^z . The velocity distribution was measured using Particle Image Velocimetry (PIV). The setup and details of both techniques were the same as in our previous work (6). The recording was carried out for 10 seconds at a time interval of 60 seconds for 20 minutes. All results in this paper were time-averaged over one second, i.e. 10 frames.

3 Results and discussions

The key result of this work is the observation of a highly reproducible bending of the fringes in the interferograms directly below the magnet after the magnet is applied to the paramagnetic solution, which is directly caused by a change of concentration in this region. This clearly indicates a change in the refractive index Δn of the solution, which may be caused by a change in either the concentration or the temperature of the solution. However, no physical reason is identifiable for the latter because the solution was safely prevented from being heated by the laser or from cooling through evaporation. Thus, we processed the interferogram packages under the assumption, that Δn is entirely caused by a change in the concentration, $C_{Mn^{2+}}$, of the Mn^{2+} ions.

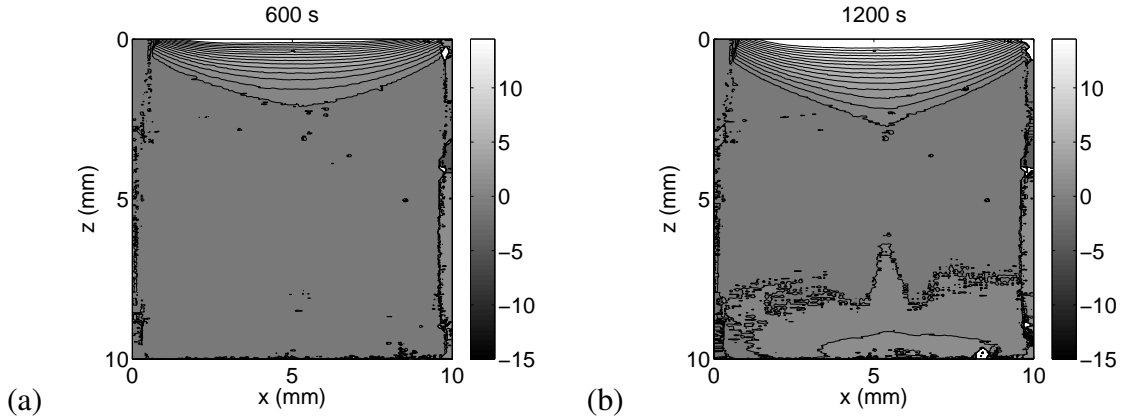


Figure 2: Iso-concentration contour plots of the 1 M $MnSO_4$ solution (a)600 s and (b) 1200 s after the magnet was applied on top of the cell. The unit in the legends is the concentration change in mM.

Fig. 2 shows the resulting contour plots representing the change in $C_{Mn^{2+}}$ for 1M $MnSO_4$ solutions at $t = 600$ and 1200 seconds after the magnet was applied. We observed the formation of a convex layer close to the magnet in which $C_{Mn^{2+}}$ is higher than in the bulk. The enrichment increases with time, cf. Fig. 2(a) and (b), to reach a steady state at $t \sim 1200$ s (Fig 2b). The larger the amount of C_0 , the stronger the concentration increase at the top, which is found to reach 2% of C_0 . The convex shape of the optical inhomogeneous layer below the magnet reproduces the convex shape of the spatial distribution of the dominant component of the magnetic field gradient force (Fig. 1d).

The origin of this increase can be understood by zooming into the concentration contour plots and applying PIV in parallel. Fig. 3a proves that there is a drainage from the enrichment layer down to the bottom center of the cell. This drainage, which feeds the increase at the bottom as visible in Fig. 2b, is associated with a downward flow visualized by the PIV measurement in Fig. 3b. The downward flow occurs in the center of the cell, i.e. at the position of maximum

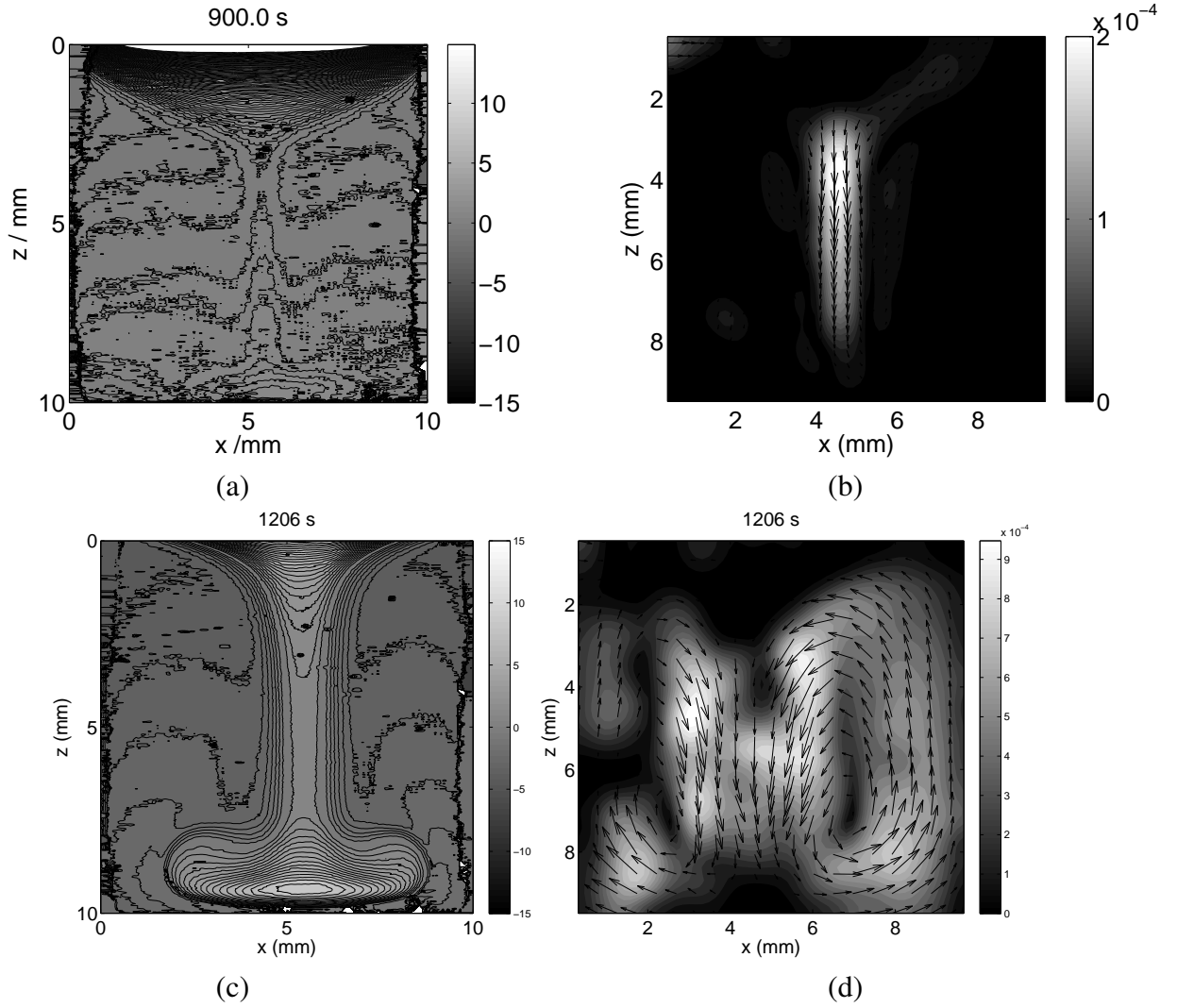


Figure 3: Iso-concentration contours (a, c) and velocity vector plots (b, d) of the solution 900 seconds after the magnet was applied on top of the cell (a and b) and 6 seconds after the magnet was removed (c and d) for the 1 M MnSO_4 .

bending of the concentration iso-contours in Fig. 3a. Thus we can infer that the steady state results from a balance between an attraction of Mn^{2+} ions towards the magnet and their depletion due to a drainage by means of a downward flow.

The next important question to be answered is that of what happens when the magnet is removed. Fig. 3 c and d show that the enriched layer on top of the cell immediately drops down to the bottom in a few seconds. This closely resembles a Rayleigh-Taylor instability which occurs when a layer of higher density is imposed on another one of lower density. The falling plume, entraining the content of the enrichment layer, can be seen well in Fig. 3c. This plume creates a downward flow in the center which is clearly visible in the PIV, Fig. 3d. By continuity, an upward flow occurs in the outer parts of the cell which replaces the fluid dragged from the enrichment layer.

This observed demixing of an initially homogeneous solution is a highly reproducible but unexpected phenomenon. Indeed, for the present case of a MnSO_4 solution in a closed system with concentrations significantly below the solubility product, one would not expect a demixing even in the presence of the applied magnetic field. Therefore, we first speculated about a parasitic

thermal effect. However, with the precautions explained above, both heating by the laser and evaporative cooling of the solution are excluded, and hence also any kind of magnetocaloric pumping. Also, no nanoparticle formation was detected using dynamic light scattering within one hour of the solution being stored under experimental conditions.

4 Conclusions

The concentration enrichment which we report above is restricted neither to the paramagnetic Mn^{2+} ions nor to SO_4^{2-} as anions. We found that similar phenomena also occur for the stronger paramagnetic Gd^{3+} or for Cl^- as an anion. By contrast, no significant effect was found for the CuSO_4 solution because χ_{sol} , and correspondingly f_m , are much smaller than in MnSO_4 . We believe that this possibility to separate paramagnetic metal ions from aqueous solutions might be of significant interests for recycling purposes.

Acknowledgements

Financial support from Deutsche Forschungsgemeinschaft (DFG) in frame of the Collaborative Research Center (SFB) 609 and by DLR (50 WM 1350) are gratefully acknowledged.

References

- [1] Pamme N.: Magnetism and microfluidics. *Lab. Chip*, 6 (2006) 24–38
- [2] Rosensweig R. E.: *Ferrohydrodynamics*. Mineola, NY: Dover Publications 1997
- [3] Monzon L.; Coey J.M.D. : Magnetic fields in electrochemistry: The Kelvin force. a mini-review. *Electrochem. Commun.* 42 (2014) 42–45
- [4] Coey J.M.D.; Aogaki R.; Byrne F.; Stamenov P: Magnetic stabilization and vorticity in submillimeter paramagnetic liquid tubes. *Proc. Natl. Acad. Sci. U.S.A.* 106 (2009) 8811–8817
- [5] Yang X.; Tschulik K.; Uhlemann M.; Odenbach S.; Eckert K.: Enrichment of paramagnetic ions from homogeneous solutions in inhomogeneous magnetic fields. *J.Phys. Chem. Lett.* 3 (2012) 3559–3564
- [6] Yang X.; Eckert K.; Muehlenhoff S.; Odenbach S.: On the decay of the lorentz-force-driven convection in vertical concentration stratification during magneto-electrolysis. *Electrochim. Acta* 54 (2009) 7056–7065